20th Australasian Fluid Mechanics Conference
Perth, Australia
5-8 December 2016

Dye Visualisation of Wake Flow around a Model Submarine at Yaw

S.-K. Lee[1,2], L. P. Erm[1] and M. B. Jones[1]

[1]Defence Science and Technology Group, Melbourne, VIC 3207 AUSTRALIA

[2]University of Tasmania, Launceston, TAS 7250 AUSTRALIA

Abstract

An earlier surface-streamer experiment on a generic "Joubert" model submarine in the Defence Science and Technology (DST) Group low-speed wind tunnel revealed complex flow patterns when the submarine is yawed up to 18°. The present study aims to discover by dye visualisation if there are similar flow patterns produced in water.

From studying the dye-flow images, the salient features are topologically consistent with those identified from earlier surface-streamer visualisation. In the topological model constructed from the dye images, the instantaneous wake of the submarine fin contains a series of interconnected vortex rings. The observed vortex shedding rate is an increasing function of the submarine yaw angle from 0° to 18°.

This dye visualisation provides an initial step towards understanding the formation of the wake structures to assist future wind-tunnel investigations on how these structures possibly evolve at increasing flow speeds, and to help identify possible key locations which can benefit from point-measurement or laser-based techniques.

Introduction

Maritime research at the DST Group makes use of a generic conventional hull form defined by Joubert [1] to study the wake of submarine flows. The study has practical relevance as the presence of shear-layer structures and their interaction with the propeller can affect propulsion and manoeuvre as well as contribute to noise and the acoustic signature. However, to conduct a wake survey is time consuming and can be expensive since the flow field needs to be mapped in detail usually by point-measurement or laser-based (planar) techniques. To gain an understanding of the underlying structures before attempting to measure the wake field, it is useful to begin by performing flow visualisation.

Lee [2] has carried out a surface-streamer visualisation study of a 1.35m-long Joubert model in the DST Group low-speed wind tunnel. The streamer results revealed turbulent separation on the leeward side of the submarine when the yaw angle is increased from 0° to 18°. The time-averaged flow [2] shown in figure 1 includes the horseshoe vortex ($\overline{F_{fp}F_jF_{fs}}$), the hull vortices ($F_{hc}$ and F_{hb}) and the fin-tip vortex (F_{ft}).

At 18° yaw, the most significant feature is a strong reattachment node (N_{fl}) on the fin. The topological model (figure 1) constructed from the streamer data [2] indicates a U-shaped vortex around this reattachment node. This U-shaped vortex consists of three segments: (i) a bound vortex which spans the height of the fin, connected to (ii) the fin-tip vortex and (iii) a vortex leg along the submarine casing. On the casing, the rotation sense of the vortex leg arising from the fin (F_{fp}) is opposite to that of the adjacent vortex leg arising from the nose (F_{hc}), and so these vortex legs tend to cancel each other [2].

This paper presents dye visualisation of the wake produced by the Joubert hull with an aim to assist future wind-tunnel testing efforts at the DST Group. For clarity of dye visualisation in water, and as an initial step towards understanding the development of the wake, the flow is tested at a low speed. The wake structure is interpreted by observing standard rules of topology [3] and the vortex law of Helmholtz [4].

Model Testing in a Water Tunnel

The Joubert [1] hull shown in figure 1 includes a bare hull of fineness ratio of 7.3 with a casing and a fin. The hull is axisymmetric for the first 7% of the body length (L), where the nose of the hull is derived from a NACA-0014.2 forebody. The fin has the shape of a NACA-0015 foil with a rounded trailing edge. The fin height is 8% L, the chord length is 16% L and the leading edge of the fin is located at 31% L. The tail cone includes a set of generic "X"-rudders as aft control surfaces. The tapering to the end of the tail cone starts at 76% L.

Details of the wake flow are obtained by performing dye visualisation on a 0.385m-long Joubert model in the DST Group water tunnel. The water-tunnel test section is 0.38m wide, 0.51m high and 1.63m long. For this test, the tail cone is trun-

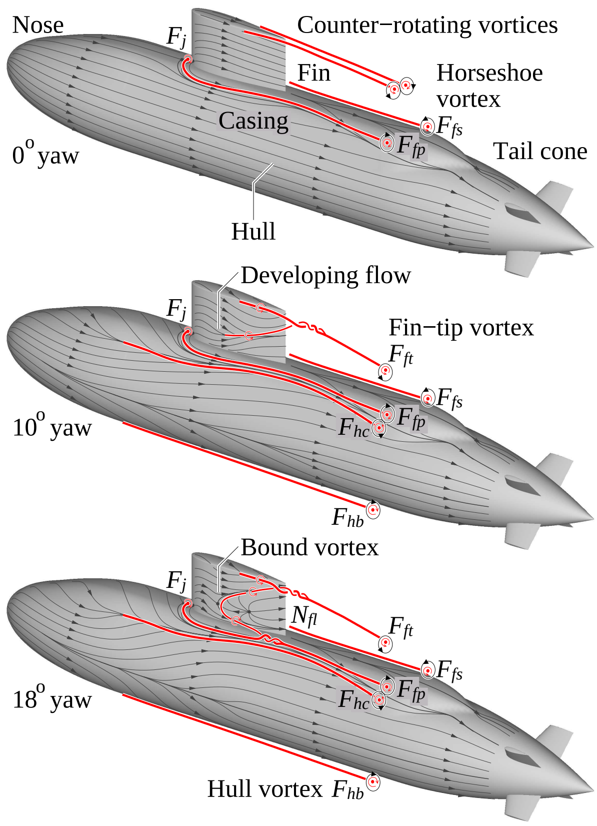

Figure 1. Time-averaged leeward flow for the Joubert model inferred from streamer visualisation in a low-speed wind tunnel [2]. Symbols: $F=$ focus, $N=$ node; subscripts: $hc=$ hull casing, $hb=$ hull base, $fp=$ fin port, $fs=$ fin starboard, $ft=$ fin tip, $fl=$ fin leeward, $j=$ junction.

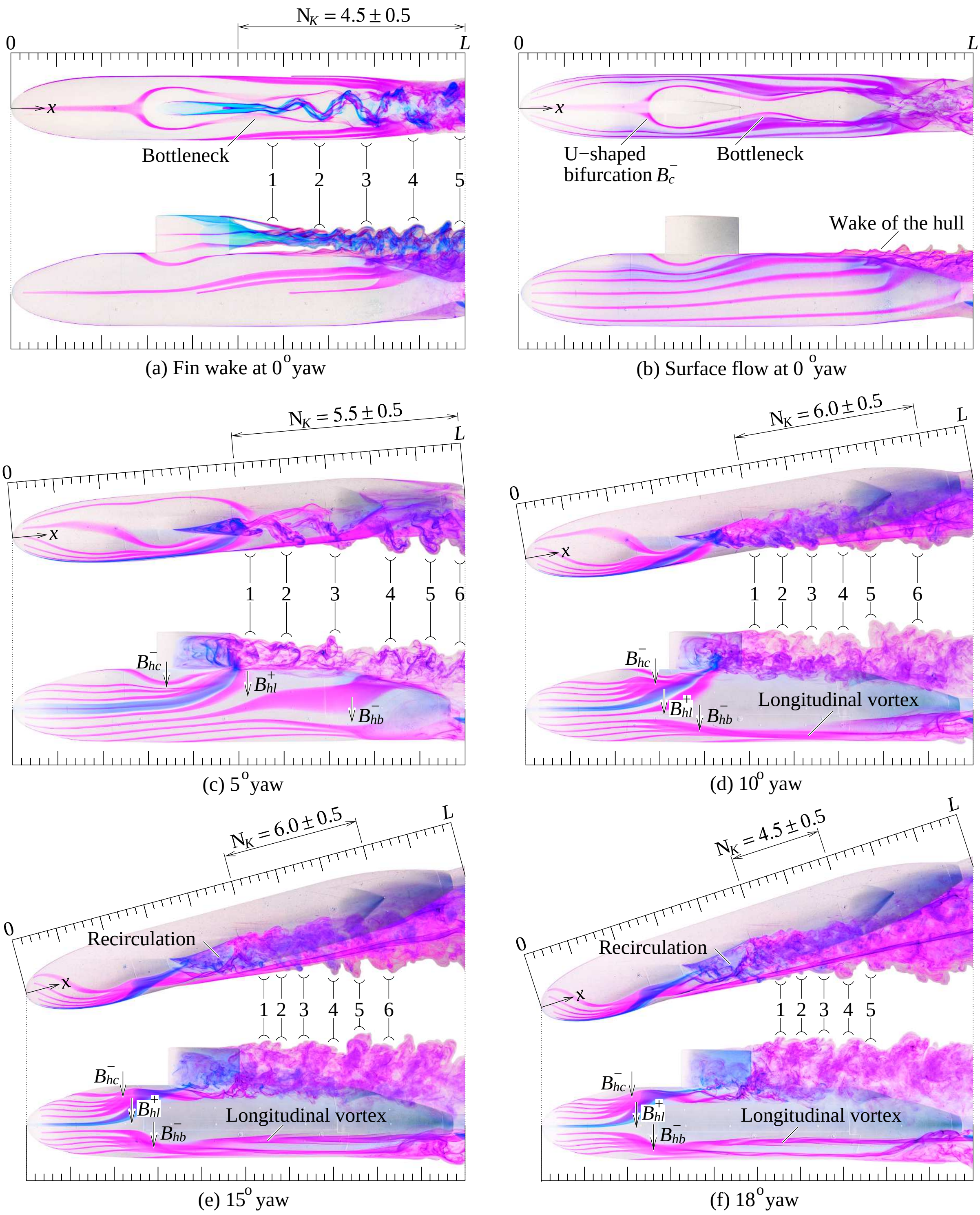

Figure 2. Examples of instantaneous flow with the Joubert model yawed towards the port side. The dye filaments are introduced from (a) selected ports on the hull and the fin, and (b-f) circumferential ports on the nose. Colour scales are inverted. Vertical arrows indicate the inception of surface bifurcations B_{hc}^-, B_{hl}^+ and B_{hb}^-. Symbol N_K denotes a number of observed Kármán vortex structures over a downstream distance (Δx) from the fin.

cated at 97% L with the aft control surfaces removed to provide an entry point for a sting support and for dye supply. For clarity, the dye filaments are introduced from selected ports (1.2mm internal diameter) distributed over the surface of the model. The free-stream is operated at a nominal speed (U_∞) of 0.1m/s. The model is attached to an automated support mechanism [5] via the sting to provide yaw motion. The yaw angles (ψ) for this test are 0°, 5°, 10°, 15° and 18°.

Instantaneous Dye-Flow Patterns

Figure 2 shows typical results from instantaneous dye visualisation, where the top- and side-view images are captured simultaneously by using two separate cameras. For the straight-ahead condition (0° yaw), the fin wake is observed by introducing dye from the fin (figure 2(a)). Introducing dye from the nose shows the streamlines on the surface of the hull (figure 2(b)).

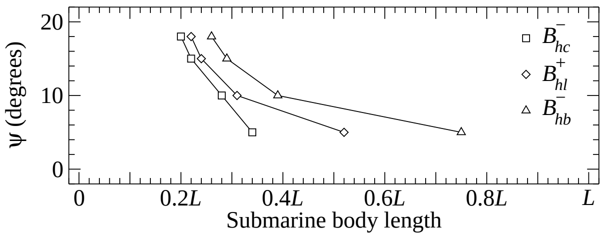

Figure 3. Locus of surface-bifurcation inception determined from dye visualisation (figure 2). Measurement uncertainty is $\sim \pm 0.04L$.

At 0° yaw, the wake of the fin is a classic Kármán vortex street (figure 2(a)). A bottleneck of streamlines just behind the fin is evidence of locally accelerated flow. Downstream of the bottleneck, visible interaction between the vortex street (in blue) and the wake of the hull (in red) occurs near the start of the tail cone.

In figures 2(b-f), the evolution of surface streamlines at increasing angle of yaw (ψ) is observed by introducing dye from circumferential ports located at the nose. As ψ is increased from 0° to 18°, the dye-flow patterns show an increasing recirculation region on the leeward side of the fin. The recirculation is so strong that dye filaments entrained toward this region are rapidly dispersed in the wake of the fin.

Bifurcation of the Surface Flow

Inspection of figure 2 shows evidence of a U-shaped negative bifurcation (B_c^-) on the casing around the base of the fin. When the model is yawed, this further produces a positive bifurcation (B_{hl}^+) on the leeward side of the hull and a negative bifurcation (B_{hb}^-) along the base of the hull. On the upper hull, the dye filaments converge on the leeward side of the casing (B_{hc}^-) before dispersing into the wake of the fin. The dye filaments bifurcating from the lower hull (B_{hb}^-) are helically twisted into a longitudinal vortex (F_{hb}). In figure 3, a plot of the locus of surface-bifurcation inception (for B_{hc}^-, B_{hl}^+ and B_{hb}^-) shows that the bifurcation inception moves upstream along the hull with increasing yaw angle (ψ).

To summarise, the dye-flow patterns (figure 2) are topologically consistent with the surface-streamer patterns (figure 1) observed in the DST Group low-speed wind tunnel [2], and they confirm a number of key flow features as follows.

- The negative bifurcation B_{hb}^- corresponds with the longitudinal vortex F_{hb} near the base of the hull.
- The U-shaped negative bifurcation B_c^- on the casing corresponds with the horseshoe vortex $\overline{F_{fp}F_jF_{fs}}$ around the fin junction.
- The strong recirculation of the fin wake is consistent with the reattachment node N_{fl} on the leeward face of the fin.

Vortex Structure of the Fin Wake

From dye visualisation, figure 1 is supplemented with a qualitative description of the instantaneous wake flow in figure 4. The following description of the flow is idealised for clarity. In reality, the onset of turbulence for example at increasing flow speeds would likely lead to a breakdown of coherent structures.

In figure 4, the idealised fin wake is described by a series of interconnected vortex rings (shown in blue) with the trajectory of these rings being in the direction of the free-stream. A fluid particle introduced into the fin wake generally meanders through the interconnected rings (shown in green). For $\psi = 0°$, the vortex rings grow symmetrically about the mirror plane of the fin. For $\psi > 0°$, the rings are distributed on the leeward side of the fin and are asymmetric due to the cross flow.

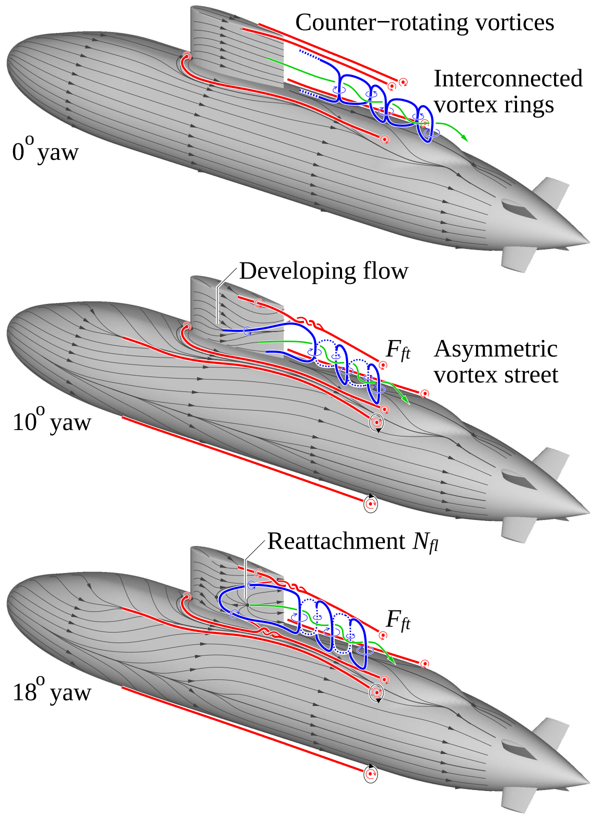

Figure 4. Instantaneous vortex structure (in blue) and streamline (in green) superimposed on the time-averaged flow (in red) from figure 1.

Figure 5 provides a schematic interpretation of the flow pattern in a horizontal slice through the vortex rings at $\psi = 0°$. On the casing, the flow pattern of the fin wake resembles a positive-bifurcation line [2]. In figure 5, this positive bifurcation (B_c^+) falls between the legs of the U-shaped negative bifurcation (B_c^-).

Figure 6 shows that by increasing the yaw angle, the shed vortices are more closely distributed on the leeward side of the fin. For $\psi > 10°$, recirculation dominates the near wake of the fin, where reattachment of the recirculated flow appears as a half saddle. This half-saddle point corresponds with the reattachment node (N_{fl}) on the leeward face of the fin (figure 4).

Further Observations: Vortex Shedding Rate

The characteristic frequency of the Kármán vortex shedding (f_K in Hz) from the fin is obtained by directly observing video footage of the dye-flow patterns (figure 2), and manually counting the number of flow structures over a period of $\simeq 1$ minute. For this experiment, the vortex-shedding rate is generally $\simeq$ 2Hz for $\psi = 0°$ up to $\simeq$ 3Hz for $\psi = 18°$.

The Strouhal number of the fin vortex shedding is expressed as

$$St_w = \frac{f_K \times w}{U_\infty}, \quad (1)$$

where w is the projected width of the fin on a plane normal to the free-stream, which approximates the near-wake thickness of the fin. Figure 7(a) shows the variation in w/L for small yaw angles of the submarine fin NACA-0015. The plot of Eq. (1) in figure 7(b) includes a line of best fit for the Strouhal number in the range $10° \lesssim \psi \lesssim 18°$, which is

$$St_w = 0.035\psi - 0.019 \quad (2)$$

with an r.m.s. error of 0.2%. The vertical error-bars indicate the

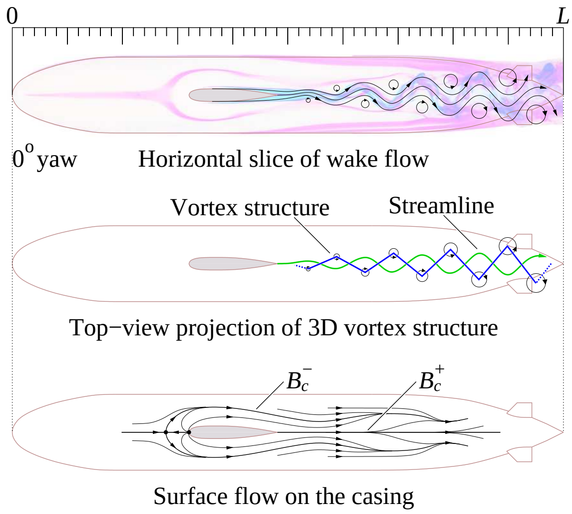

Figure 5. Schematic interpretation of wake flow from figure 2(a). Dye image is watermarked. B_c^- is a U-shaped negative bifurcation around the fin. B_c^+ is a positive bifurcation downstream of the fin.

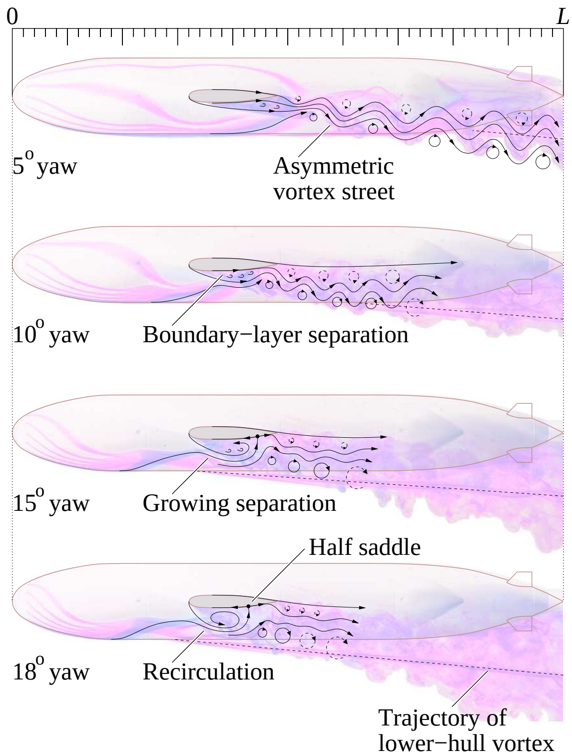

Figure 6. Schematic interpretation of wake flow from figures 2(c-f). Dye images are watermarked.

limits of departure from the mean values based on uncertainty in the number of observed flow structures.

For $\psi = 0^\circ$, the fin wake has minimal interaction with the surface flow over the hull, and the Strouhal number St_w is close to $1/2\pi$ for near-wake vortex shedding from foils [6]. As ψ is increased up to 10°, the boundary layer over the fin generally separates with no visible reattachment (figure 6). By further increasing the yaw angle in the range $10^\circ \lesssim \psi \lesssim 18^\circ$, the fin begins to interact strongly with the flow separating from the casing, and the observed shedding frequency becomes directly proportional to the submarine yaw angle (figure 7).

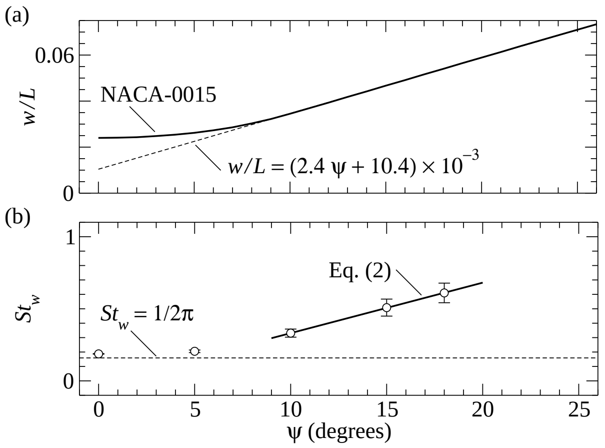

Figure 7. Scaling of the submarine NACA-0015 fin vortex shedding rate (○) as a function of yaw angle (ψ).

Concluding Remarks

From dye visualisation of the Joubert model submarine in water, the authors have observed that the flow patterns are topologically similar to those identified in the DST Group low-speed wind tunnel [2]. The dye-flow patterns, like the surface streamers, show strong surface bifurcation on the leeward side of the hull. The inception of the surface bifurcation moves upstream of the hull with increasing submarine yaw angle.

Downstream of the submarine fin, the wake displays a classic Kármán vortex street. In the constructed topological model of the flow, this vortex street is representative of a horizontal slice of a series of interconnected vortex rings. The Strouhal number of vortex shedding is directly proportional to the yaw angle from $\sim 10^\circ$ to 18°. Further details of the wake flow, including the behaviour of vortex shedding at increasing flow speeds (i.e. the effect of Reynolds number), is a subject of continuing experimental investigation.

Acknowledgement

The authors offer their sincere thanks to Brian Crowley for the dye-visualisation photography and to Gregory Seil, Matteo Giacobello and Dev Ranmuthugala for helpful discussions.

References

[1] Joubert, P. N. Some aspects of submarine design part 2: shape of a submarine 2026. TR1920, DSTO, 2006.

[2] Lee, S.-K. Topology model of the flow around a submarine hull form. TR3177, DST Group, 2015.

[3] Flegg, H. G. *From geometry to topology*. The English Universities Press Ltd., London, 1974.

[4] Helmholtz, H. LXIII. On integrals of the hydrodynamical equations, which express vortex-motion. *Philosophical Magazine Series 4*, 1867, 33(226):485–512.

[5] Erm, L. P. Development and use of a dynamic-testing capability for the DSTO water tunnel. TR1836, DSTO, 2006.

[6] Blake, W. K. *Mechanics of flow-induced sound and vibration, vol. 2: complex flow-structure interactions*. Academic Press, New York, 1986.